Ludmila Krejcova[1]
Dana Dospivova[1]
Marketa Ryvolova[1,2]
Pavel Kopel[1,2]
David Hynek[1,2]
Sona Krizkova[1,2]
Jaromir Hubalek[1,2]
Vojtech Adam[1,2]
Rene Kizek[1,2]

[1]Department of Chemistry and Biochemistry, Faculty of Agronomy, Mendel University in Brno, Czech Republic, European Union
[2]Central European Institute of Technology, Brno University of Technology, Czech Republic, European Union

Received April 15, 2012
Revised July 2, 2012
Accepted July 3, 2012

Research Article

Paramagnetic particles coupled with an automated flow injection analysis as a tool for influenza viral protein detection

Currently, the influenza virus infects millions of individuals every year. Since the influenza virus represents one of the greatest threats, it is necessary to develop a diagnostic technique that can quickly, inexpensively, and accurately detect the virus to effectively treat and control seasonal and pandemic strains. This study presents an alternative to current detection methods. The flow-injection analysis-based biosensor, which can rapidly and economically analyze a wide panel of influenza virus strains by using paramagnetic particles modified with glycan, can selectively bind to specific viral A/H5N1/Vietnam/1203/2004 protein-labeled quantum dots. Optimized detection of cadmium sulfide quantum dots (CdS QDs)-protein complexes connected to paramagnetic microbeads was performed using differential pulse voltammetry on the surface of a hanging mercury drop electrode (HMDE) and/or glassy carbon electrode (GCE). Detection limit (3 S/N) estimations based on cadmium(II) ions quantification were 0.1 μg/mL or 10 μg/mL viral protein at HMDE or GCE, respectively. Viral protein detection was directly determined using differential pulse voltammetry Brdicka reaction. The limit detection (3 S/N) of viral protein was estimated as 0.1 μg/mL. Streptavidin-modified paramagnetic particles were mixed with biotinylated selective glycan to modify their surfaces. Under optimized conditions (250 μg/mL of glycan, 30-min long interaction with viral protein, 25°C and 400 rpm), the viral protein labeled with quantum dots was selectively isolated and its cadmium(II) content was determined. Cadmium was present in detectable amounts of 10 ng per mg of protein. Using this method, submicrogram concentrations of viral proteins can be identified.

Keywords:
Electrochemical detection / Hemagglutinin / Influenza / Magnetic separation / Voltammetry
DOI 10.1002/elps.201200304

1 Introduction

Influenza represents one of the greatest threats in society today. It is not surprising that the World Health Organization (WHO) initiated the Global Influenza Program, which provides member states with strategic guidance, technical support, and coordination of activities essential to better prepare healthcare systems against seasonal, zoonotic, and pandemic influenza threats to populations and individuals (http://www.who.int/influenza/en/) [1, 2]. According to WHO, seasonal influenza is responsible for several million cases of acute illnesses and between 250 000 and 500 000 deaths each year [3].

There are three genera of the influenza virus: Influenza virus A, Influenza virus B, and Influenza virus C. They are RNA viruses that make up three of the five genera of the *Orthomyxoviridae* family. Type A virus, the most virulent human pathogens among the three influenza types, causes the most severe disease. This virus can be further subdivided into different serotypes based on antibody responses. The influenza virus contains two major surface proteins: hemagglutinin (HA) and neuraminidase. HA mediates glycan receptor binding and membrane fusion for viral entry. Neuraminidase conducts receptor-destroying enzyme activity important for virus release [4]. Subtypes of influenza viruses are classified according to these proteins [5, 6].

More than 500 cases of avian H5N1 influenza infections in humans have been reported from 15 countries, of which nearly 60% have resulted in death (Fig. 1). Recently published meta-analysis in Science shows 12 677 participants in 20 studies that have been infected with the avian H5N1 have mild

Correspondence: Professor Rene Kizek, Department of Chemistry and Biochemistry, Mendel University in Brno, Zemedelska 1, CZ-613 00 Brno, Czech Republic
E-mail: kizek@sci.muni.cz
Fax: +420-5-4521-2044

Abbreviations: **CdS QDs**, cadmium sulfide quantum dots; **FIA**, flow injection analysis; **GCE**, glassy carbon electrode; **HA**, hemagglutinin; **HMDE**, hanging mercury drop electrode; **QD**, quantum dots; **WHO**, World Health Organization

Colour Online: See the article online to view Figs. 1–8 in colour.

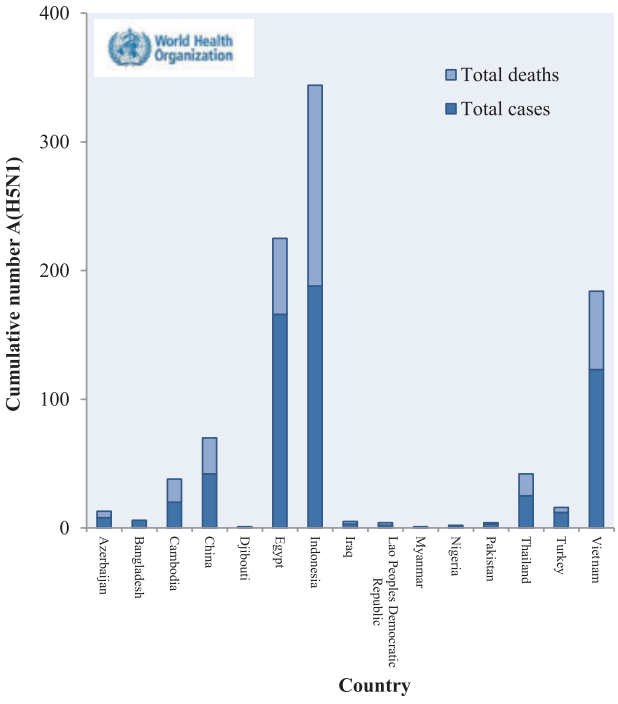

Figure 1. Affected areas with confirmed cases of H5N1 avian influenza since April 5, 2003, modified according to http://www.who.int/influenza/human_animal_interface/avian_influenza/en/.

symptoms or subclinical infections that are not currently accounted for; thus, the true fatality rate for H5N1 influenza viruses is likely to be less than the frequently reported rate of more than 50% [7]. It is possible that deaths caused by H5N1 infections, as documented by WHO, are also underestimated. A portable and robust standardized approach for large-scale studies is examined.

Nanoparticles have numerous possible applications in biosensors and bioassays. Electrochemical biosensors and bioassays have attracted considerable interest due to their high performance, miniaturized construction, and low cost [8]. Conventional enzyme and electroactive labels have incorporated nanoparticles, nanotubes, and nanowires due to their improved sensitivity in small molecule and protein detection. Gold nanoparticles electrodes used to build immunosensors were the first target materials studied in electrochemical immunosensors and DNA biosensors [9–11]. Semiconductor nanoparticles, inorganic compounds, and apoferritin or liposomes-labeled complexes can be applied as electrochemical targets for bioassays. Semiconductor nanoparticles also called quantum dots are of particular interest because of their size and tuneable fluorescence emission. Owing to their unique properties, semiconductor nanoparticles have generated considerable interest for optical biodetection. The intrinsic redox properties and sensitive electrochemical stripping analysis of the metal components of semiconductor nanoparticles cause labels in the electrochemical biosensors to be very sensitive; thus, low detection limits can be achieved. Liu et al. introduced an electrochemical immunoassay protocol for simultaneously measuring multiple protein targets based on the use of CdS, ZnS, and PbS quantum dots (QDs). Each protein gives a distinct voltammetric peak whose position and size reflects the identity and amount of the corresponding antigen with fmol detection limits [12, 13].

This study aimed to develop a low-cost isolation and rapid CdS quantum dots-based biosensor to detect viruses. Viral quantity was determined through cadmium(II) ion concentrations abstracted from quantum dots. The results were confirmed by differential pulse voltammetry Brdicka reaction. Particular attention was focused on the application of streptavidin-coated paramagnetic particles modified with biotinylated glycan and its selective binding properties to the influenza virus.

2 Materials and methods

2.1 Chemicals

Tris(2-carboxyethyl)phosphine was from Molecular Probes (Eugene, OR, USA). $Co(NH_3)_6Cl_3$ and other chemicals used were purchased from Sigma Aldrich (St. Louis, MA, USA) unless otherwise noted. Stock solutions were prepared from ACS water. pH value and conductivity was measured using inoLab Level 3 (Wissenschaftlich-Technische Werkstatten; Weilheim, Germany). Deionized water underwent demineralization by reverse osmosis using Aqua Osmotic 02 (Aqua Osmotic, Tisnov, Czech Republic) and was subsequently purified using Millipore RG (MilliQ water, 18 MΩ, Millipore, Billerica, MA, USA). Deionized water was used for rinsing, washing, and buffer preparation.

2.2 Preparation of CdS QDs

CdS QDs were prepared using a slightly modified version of a published method [14]. Cadmium nitrate tetrahydrate $Cd(NO_3)_2 \cdot 4H_2O$ (0.1 mM) was dissolved in ACS water (25 mL). A 3-mercaptopropionic acid (35 μL, 0.4 mM) was slowly added to the stirred solution. Afterward, the pH was adjusted to 9.11 with 1 M NH_3 (1.5 mL). Sodium sulfide monohydrate $Na_2S{\cdot}9H_2O$ (0.1 mM) in ACS water was poured into the solution while vigorously stirring. The acquired yellow solution was stirred for 1 h. Prepared CdS-quantum dots were stored in the dark at 4°C.

2.3 Preparation of samples

A/H5N1/Vietnam/1203/2004 protein (accession no. ISDN 38687, Prospec-Tany TechoGene, Tel Aviv, Israel) (200 μL, 100 μg/mL) was mixed with a solution of CdS QDs (100 μL). This mixture was shaken for 24 h at room temperature (Vortex Genie2 [Scientific Industries, Bohemia, NY, USA]). The volume of solution was reduced to 100 μL on an Amicon

Ultra 3k centrifugal filter device (Millipore). Centrifuge 5417R (Eppendorf, Hamburg, Germany) was performed under the following parameters 15 min, 6000 rpm, 20°C. The obtained concentrate was diluted with 400 μL of ACS water and reduced on centrifuge to 100 μL. The process was repeated five times. The washed sample was diluted to 300 μL and used for succeeding measurements.

2.4 Magnetic nanoparticle separation

Streptavidin Dynabeads M-270 was purchased from Life Technologies (Carlsbad, CA, USA). Biotinylated multivalent glycans (01–078 [Neu5Acα2–3Galβ1–3GlcNAcβ1-PAA-biotin]) were obtained from GlycoTech (Gaithersburg, MD, USA). Soluble forms of HA derived from newly emerging influenza viruses expressed in baculovirus, were purchased from Prospec-Tany TechnoGene. Streptavidin Dynabeads M-270 (10 μL) was pipetted to microplates (PCR 96, Eppendorf), then subsequently transferred to a magnet plate. Stored solution was drained from the magnetic particles. Magnetic particles were washed three times with 100 μL of phosphate buffer (0.3 M, pH 7.4, made from NaH_2PO_4 and Na_2HPO_4). Twenty microliters of biotinylated glycan were added to each of the wells and incubated (30 min, 25°C, 400 rpm). After the incubation, the sample was washed three times with phosphate buffer (0.3 M, pH 7.4). Subsequently 20 μL of H5N1-Cd-labeled protein was added. It was further incubated (30 min, 25°C, 400 rpm) and washed with 100 μL of phosphate buffer (0.3 M, pH 7.4). Thirty-five microliters of phosphate buffer (0.3 M, pH 7.4) was added followed by the treatment of ultrasound needle (2 min). The plate was transferred to the magnet plate and the supernatant (product) was measured using differential pulse voltammetry. The detected substance was identified as cadmium (quantum dots).

2.5 Determination of proteins by Brdicka reaction

Differential pulse voltammetric measurements were performed with a 747 VA Stand instrument connected to a 693 VA Processor and 695 Autosampler (Metrohm, Herisau, Switzerland). It was equipped with a standard cell consisting of three electrodes, a cooled sample holder, and a measurement cell set at 4°C (Julabo F25, JulaboDE, Seelbach, Germany). The three-electrode system consisted of a hanging mercury drop electrode (HMDE) with a drop area of 0.4 mm^2 as the working electrode, an Ag/AgCl/3M KCl reference electrode, and a platinum electrode acting as the auxiliary. VA Database 2.2 by Metrohm was used for data acquisition and subsequent analysis. The analyzed samples were deoxygenated prior to measurements by purging with argon (99.999%) saturated with water for 120 s. Brdicka-supporting electrolyte containing 1 mM $Co(NH_3)_6Cl_3$ and 1M ammonia buffer (NH_3(aq) + NH_4Cl, pH = 9.6) was used. The supporting electrolyte was exchanged after each analysis. The parameters of the measurement were as follows: initial potential of −0.7 V, end potential of −1.75 V, modulation time 0.057 s, time interval 0.2 s, step potential 2 mV, modulation amplitude −250 mV, E_{ads} = 0 V. The volume of injected sample was 5 μL with a total volume of 2 mL in the measurement cell (5 μL of sample + 1995 μL Brdicka solution).

2.6 Electrochemical determination of cadmium

Determination of cadmium by differential pulse voltammetry was performed using a 663 VA Stand (Metrohm) and a standard cell with three electrodes. The three-electrode system consisted of an HMDE with a drop area of 0.4 mm^2 as the working electrode, an Ag/AgCl/3M KCl reference electrode, and a glassy carbon acting as the auxiliary electrode. GPES 4.9 software was employed for data processing. The analyzed samples were deoxygenated prior to measurements by purging with argon (99.999%). Acetate buffer (0.2 M CH_3COONa + CH_3COOH, pH 5) was used as a supporting electrolyte. The supporting electrolyte was replaced after each analysis. The parameters of the measurement were as follows: purging time 120 s, deposition potential −0.9 V, accumulation time 240 s, equilibration time 5 s, modulation time 0.057 s, interval time 0.2 s, initial potential −0.9 V, end potential −0.3 V, step potential 0.00195 V, modulation amplitude 0.02505 V, volume of injected sample: 10 μL, volume of measurement cell 1 mL (10 μL of sample; 990 μL acetate buffer).

2.7 Flow injection analysis (FIA)

An automated FIA system with electrochemical detection was proposed. The system consisted of a solvent delivery automated analytical syringe operating in a working volume of 1–50 μL, with variable speeds ranging from 1.66 to 50 μL/s (Model eVol, SGE Analytical Science, Kiln Farm Milton Keynes, UK), a 3-way 2-position selector valve (made from 6-way valve) (Valco Instruments, Schenkon, Switzerland), and a dosing capillary that directly entered the electrochemical flow cell (CH Instruments, Austin, TX, USA). To prepare a fully automated system, a switching valve that enabled alternating between the off waste and sample flow was placed in the system. The sample (10 μL) was injected by an automated syringe (SGE Analytical Science) through a flow cell at a speed of 1.66 μL/s. The flow cell was first rinsed clean with 200 μL of ethanol in water (75% *v*/*v*), then with 200 μL of 100% ethanol, and stabilized with 200 μL of supporting electrolyte. Cleaning procedures were applied after every 50 measurements. The electrochemical flow cell includes a low volume (1.5 μL) flow-through analytical cell (CH Instruments, Austin, TX, USA), which consisted of a doubled glassy carbon working electrode, Ag/AgCl reference electrode, and an output steel tubing as an auxiliary electrode. An electrochemical flow cell was connected to a miniaturized control module, potentiostat 910 PSTAT mini (Metrohm). The differential pulse

voltammetry was used as the measuring method with the following parameters: initial potential −1.2 V, end potential −0.2 V, modulation amplitude 0.05 V, step potential 0.001 V. Acetate buffer (0.2 M, pH 5) was used as the supporting electrolyte. Each sample solution of 10 μL was diluted in acetate buffer. The data obtained were processed by the PSTAT software 1.0 (Metrohm). The experiments were carried out at 20°C.

2.8 Fluorescence measurement

Fluorescence spectra were acquired by a multifunctional microplate reader called Tecan Infinite 200 PRO (TECAN, Männedorf, Switzerland). The excitation wavelength was set at 350 nm and the fluorescence scan was measured every 5 nm within a 400 to 850 nm wavelength range. Each intensity value was based on an average of five repeated measurements. The detector gain was set at 100. The sample (50 μL) was placed in a transparent 96-well microplate with a flat bottom (Nunc). Fluorescence monitoring was performed using In vivo Xtreme system by Carestream (Rochester, NY, USA). This instrument was equipped with a 400 W xenon light source and 28 excitation filters (410–760 nm). The emitted light is captured by a 4MP CCD camera. The excitation wavelength was set at 410 nm and the emission was measured at 700 nm. The exposition time was 4.5 s. Sample volumes of 25 μL were placed in microtitrate plates (Eppendorf).

2.9 Robotic pippeting station

Computer controlled automated pipetting station, Ep-Motion 5075 (Eppendorf) was used for automated sample handling prior to electrochemical analysis. Positions C1 and C4 were thermostated (Epthermoadapter PCR96). At position B1, module reservoir for washing solutions and waste were placed. Tips were placed in positions A4 (ePtips 50), A3 (ePtips 300), and A2 (ePtips 1000). Transfer was ensured by a robotic arm with pipetting adaptors (TS50, TS300, TS1000–numeric labeling refers to maximal pipetting volume in μL) and a gripper for platform transport (TG-T). The program sequence was edited and the station was controlled in pEditor 4.0. For sample preparation, two platforms were used. A thermorack for 24 × 1.5–2 mL microtubes (Position C3) was used to store working solutions and a 96-well DPW (low binding DNA) thermostated plate with a well volume of 200 μL (Position C1) was also available. After separation, the magnetic particles were forced apart using a Promega magnetic pad (Promega, Madison, WI, USA) (position B4). The solutions were then transferred to a new DPW plate.

2.10 Descriptive statistics

Data were processed using MICROSOFT EXCEL (Microsoft, Redmond, WA, USA) and STATISTICA.CZ Version 8.0 (StatSoft CR, Prague, Czech Republic). The results are expressed as mean ±SD unless otherwise noted. The detection limits (3 S/N) were calculated according to Long and Winefordner [15], whereas *N* was expressed as a standard deviation of noise determined in the signal domain unless otherwise stated.

3 Results and discussion

At the beginning of 2009, the influenza A (H1N1) virus emerged and spread to most parts of the world. WHO considered this virus a potentially dangerous strain that could lead to a pandemic with high mortality. Transmission of swine H1N1 virus into the human population probably occurred due to changes in HA and their sialyl glycan-based receptors. Other contributing factors include its distribution in tissues of different species, host range, and tissue tropism and its capacity to initiate a human pandemic. Based on previous studies, H5N1 consists of homology-based HA-glycan structural complexes with human-type oligosaccharide receptors (*N*-acetylneuraminic acid α2–6-linked to galactose) and avian-type (*N*-acetylneuraminic acid α2–3-linked to galactose) [16–21]. However, these receptors and interactions can also be used as tools for successful isolation of various types of influenza viruses [22]. Current studies attempted to design a biosensor, which consists of paramagnetic particles-based isolation of viral proteins modified with QDs and subsequent electrochemical detection of both protein and QDs as a new type of labeling.

3.1 Characterization of QD labeling

Aqueous CdS QDs displayed long lifetimes accompanied by excellent stability [14]. The current study affirmed the stability of synthesized CdS QDs longer than 1 month. The emission spectrum of CdS QDs is shown (green line) in Fig. 2A with

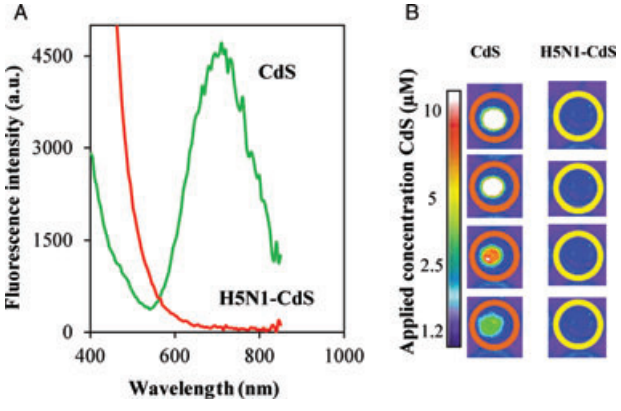

Figure 2. (A) Fluorescence intensity of CdS QD (green line) and complex H5N1-CdS (red line), excitation wavelength was 350 nm. (B) Picture of CdS QDs fluorescence (orange rings) and complex H5N1-CdS (yellow rings) measured on In vivo Xtreme system. Presented position creates concentration line in half part dilution.

an emission maximum at 710 nm. Moreover, it was found that the interaction of CdS QDs with H5N1 (red line) caused significant fluorescence quenching within the 560–850 nm range. In vivo imaging was utilized to confirm increasing concentrations of CdS QDs, which resulted in higher fluorescence intensity (Fig. 2B). The increasing fluorescence intensity of CdS QDs with corresponding increasing QDs concentrations (1.2–10 μM) are shown in Fig. 2B. The relative intensity scale is added designating the white color as of highest intensity. Fluorescence quenching after QDs interaction with H5N1 was observed. No fluorescence was detected after the interaction (H5N1-CdS, Fig. 2B). The results of gradual fluorescence quenching suggest there is a very strong interaction between CdS QDs and viral proteins apparently through disulfide bonds with free protein sulfhydryl groups (CdS-S-viral protein) and/or via binding of cadmium(II) atoms with cysteine, histidine, or lysine. Observed effects conclude the CdS quantum dot–protein interaction is strong and significant enough to be further used for other processes and applications.

3.2 Determination of cadmium(II) ions at mercury and glassy carbon electrode (GCE)

For quantification purposes, the determination of the presence of formed CdS QDs and proteins complexes by electrochemical quantification of cadmium(II) ions is advantageous in that electro-analysis of metal ions is a sensitive and robust technique routinely used for various types of real sample analysis [23, 24]. Differential pulse voltammetry was used in cadmium(II) ion detection. Two types of working electrodes were tested. HMDE was used for standard purposes. The obtained dependence was linear within a 0.1–100 μM range as follows: $y = 1.6958x$; $R^2 = 0.9911$, $n = 5$, RSD = 4.8. An automated FIA system in combination with electrochemical detection and miniaturized micropotentiostat for detection of cadmium(II) ions [25] was suggested. Cadmium(II) ions within the same concentration interval as HMDE were detected at a GCE in the presence of acetate buffer (pH 5.0). When cadmium(II) ions were detected using FIA technique coupled with GCE (FIA-GCE), well repeatable responses were obtained with the following calibration equation $y = 0.7710x - 0.2621$, $R^2 = 0.9982$, $n = 5$, RSD = 6.3. Both working electrodes were tested and cadmium(II) ions were quantified at the synthesized QDs. The obtained signals of cadmium(II) ions were recalculated to a concentration according to the calibration dependences mentioned above. HMDE calibration dependence was strictly linear within the whole tested concentration range up to 100 μM; however, GCE dependence was of quadratic course. Thus, the correlation of both dependences within the concentration interval 0.25 μM to 30 μM of cadmium(II) ions was tested. The correlation of both methods was favorable with R^2 exceeding 0.99; however, the sensitivity of GCE to cadmium(II) ions was 30% lower than HMDE.

Based on our findings, both HMDE and GCE can be utilized for QDs quantification. Therefore, interest in whether these electrodes could be utilized for quantification of CdS QDs-viral protein complexes was further examined. Viral proteins (A/H5N1/Vietnam/1203/2004; 100 μg/mL) were incubated in the presence of CdS (for other experimental conditions, see Section 2). The modified protein was purified and the unbound CdS was removed. Based on fluorimetric analysis, which confirmed QDs-viral protein complexes (Fig. 2), studies were attempted to determine the complexes through cadmium(II) ions content using differential pulse voltammetry at HMDE and GCE. The following protein concentrations (from 0.5 to 45 μg/mL) were applied to CdS QDs. Typical dependence of cadmium(II) concentration on protein concentration incubated with CdS QDs and measured at HMDE and/or GCE are shown in Fig. 3A and B, respectively. Dependence measured at HMDE had strictly linear characteristics ($y = 0.2871x$, $R^2 = 0.9973$, $n = 5$, RSD 2.1%). The observed voltammetric signals were

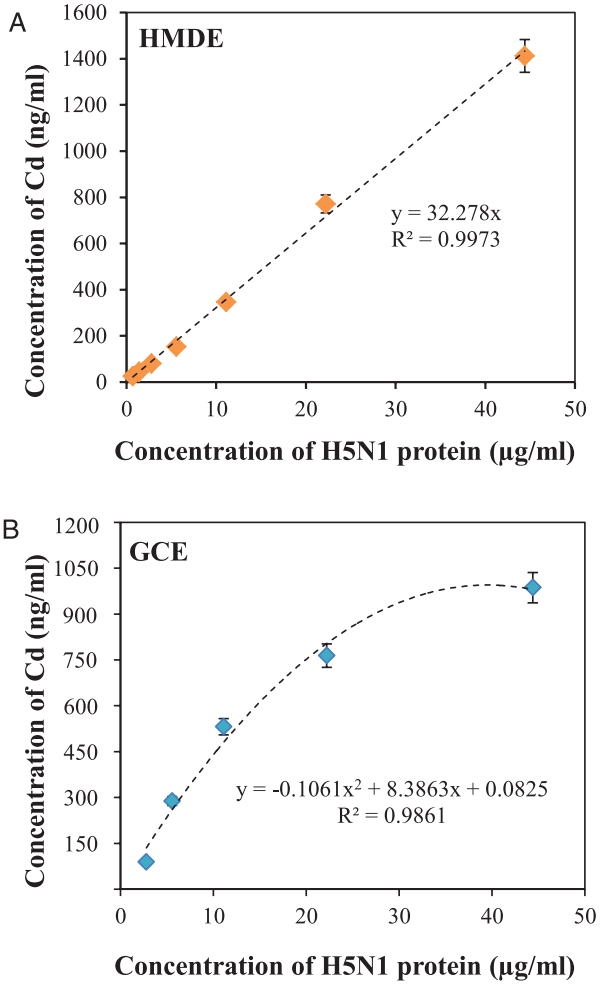

Figure 3. Dependences of cadmium ions concentration (related to protein amount) on various concentrations of complex H5N1-CdS (1: 100; 2: 50; 3: 25; 4: 12.5; 5: 6.2; 6: 3.1 7: 1.0 μM measured at (A) HMDE and (B) and FIA-GCE.

well developed and distinguishable at potential −0.6 V. Moreover, ratio of cadmium content in the formed complexes was calculated. There were approximately 20 cadmium(II) ions per complex. The ability to detect cadmium based on an indirect approach of detecting QDs-protein complexes shows great promise and pertinence. Based on obtained results, the detection limit for viral protein (3 S/N) was estimated as 0.1 μg/mL. The FIA-GCE exhibited nonlinear dependence. A mathematical approach in the form of a quadratic function (RSD 4.8%) determined protein concentration. In spite of the nonlinear dependence, the ratio of cadmium content in QDs-protein complexes demonstrated a repeated value of 20:1. The detection limit (3 S/N) of viral protein was estimated as 1 μg/mL. Both estimated detection limits pertain to real concentrations of cadmium ions that could be detected when analyzing protein-modified QDs.

3.3 Analysis of CdS QDs viral proteins complex

In addition to detecting cadmium(II) ions, this study investigated the presence of complexes in relation to viral proteins. Differential pulse voltammetry Brdicka reaction, a highly sensitive technique, was utilized to detect Cd QDs-protein complexes [26, 27]. The reaction's mechanism is based on the catalytic evolution of hydrogen on mercury electrodes from protein solutions containing SH groups in ammonia buffer and hexaamminecobalt chloride complexes ($Co(NH_3)_6Cl_3$) [28]. The mechanism of the reaction is annotated in detail, but it is believed that the cobalt(II) protein, peptide, and basic nitro compounds play important roles in the catalytic process. This method is highly recommended for sensitive analysis of peptides and proteins [29]. Communication between cobalt(II) ions and protein causes a decrease in cobalt peak and the occurrence of two new voltammetric peaks between

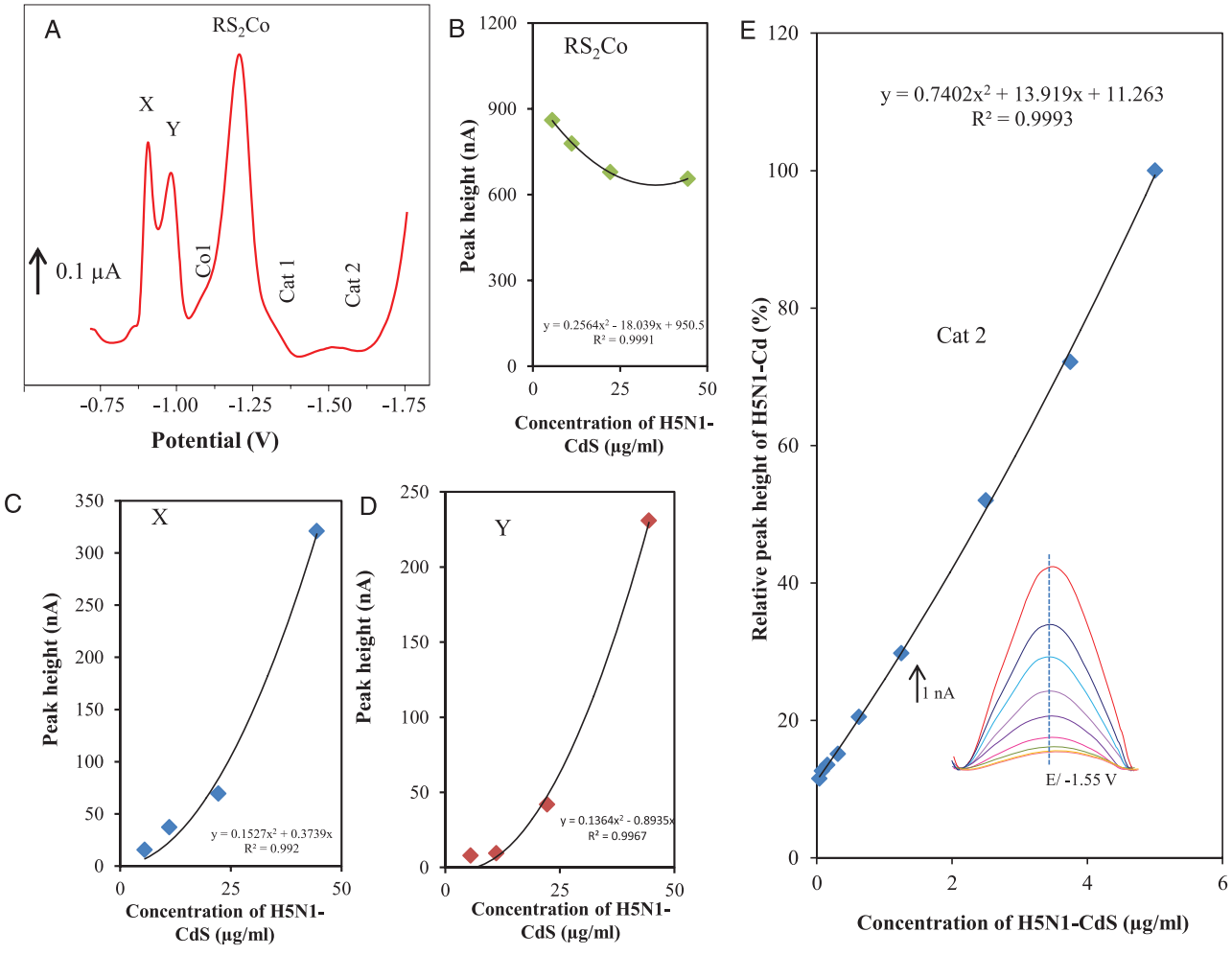

Figure 4. (A) Typical differential pulse Brdicka voltammogram of H5N1-CdS (10 μg/mL protein). Dependences of heights of (B) RS2Co, (C) signal X and (D) signal Y on concentration of H5N1-CdS QDs complex. (E) Dependences of Cat2 peak height on concentration of H5N1-CdS QDs complex; in inset: typical catalytic signal Cat2. The parameters of the measurement were as follows: initial potential of −0.7 V, end potential of −1.75 V, modulation time 0.057 s, time interval 0.2 s, step potential 2 mV, modulation amplitude −250 mV, E_{ads} = 0 V, volume of sample: 5 μL.

−1.2 and −1.5 V. The reduction of complex $R(SH)_2$ and Co(II) at potential −1.35 V corresponds to the first catalytic signal (RS_2Co). Cat1 and Cat2 signals correspond to the reduction of hydrogen at the mercury electrode. These two signals can be used to quantify complexes because height is proportional to the concentration of protein. In addition, the signal, Co1, could occasionally result from the reduction of $[Co(H_2O)_6]^{2+}$ [30]. Under current conditions, formation of catalytic signals was present between −1.0 and −1.1 V for first catalytic signal (RS_2Co) and −1.2 and −1.5 V for Cat1 and Cat2 signals, respectively (Fig. 4A). Varied strength of signal Co1 was observed at potential −0.8V. Dependence of the RS_2Co peak height on viral protein concentration is shown in Fig. 4B. Results clearly show peak height decreased with the increasing concentrations of viral protein. This phenomenon is the best explained with the formation of a complex between an SH group, Brdicka solution (cobalt ions), and CdS QD. Along with standard Brdicka peaks, two new peaks labeled X and Y were present owing to the complex formation between CdS QDs and viral protein's -SH groups. This was apparent from the obtained dependences on the concentration of protein, which are shown in Fig. 4C and D. From an analytical point of view, Cat2 is the most important detected signal. The signal increased with increasing concentrations of protein, which is shown in Fig. 4E. The detection limit (3 S/N) of viral protein was estimated as 100 ng/mL (more details will be published elsewhere).

3.4 Magnetic particles for viral isolation

The isolation procedure utilized a microfluidic instrument to perform paramagnetic particle detection. Similar approaches have implemented microfluidic platforms that can detect pathogenic avian influenza virus H5N1 in a throat swab sample. The technique coupled with polymerase chain reaction uses magnetic forces to manipulate a free droplet containing superparamagnetic particles [31–33]. These approaches are so sensitive, as Mizutani et al. showed, that they were able to isolate five particles from the influenza virus [34]. Magnetic particles can also be used for viral infection characterization. Virion immunosorting with magnetic nanobeads is direct, efficient, and adaptable to viral characterization at a nanometric resolution [35]. Another approach involved an immunomagnetic bead-based microfluidic system. By performing a simple two-step diagnostic process that includes a magnetic bead-based fluorescent immunoassay and an endpoint optical analysis the technique allows rapid detection of influenza A virus. Influenza A was targeted with magnetic particles and then labeled with a fluorescent signal

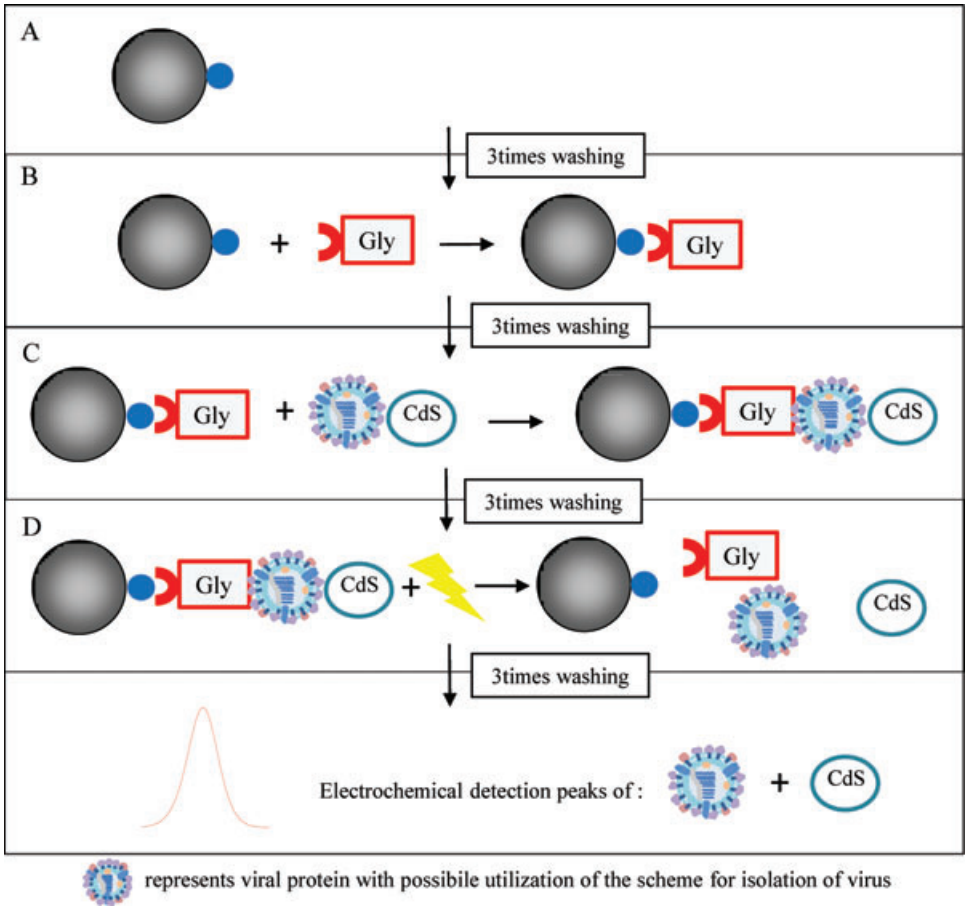

Figure 5. Scheme of a fully automated method of detection H5N1 using paramagnetic-based isolation and QD-based detection. (A) Paramagnetic streptavidin-modified particles are prepared by washing in buffer. (B) Biotinylated glycan binds to paramagnetic streptavidin-modified particles due to biotin-streptavidin affinity [45,46]. (C) Preparation of complex of CdS QDs-viral protein with the paramagnetic particles. (D) Washing and releasing of protein and cadmium(II) ions from the particles using ultrasonic pulse. (E) Electrochemical detection of HA protein and Cd.

using mAb with R-phycoerythrin [36]. Taking advantage of the large surface area-to-volume ratio, antibody-conjugated magnetic nanoparticles can act as an effective probe to extract influenza virus for gel electrophoresis and on-bead mass spectrometric analysis [37]. An approach describing sandwich design hybridization probes consisting of magnetic particles and quantum dots with target DNA, and their application in the detection of avian influenza virus (H5N1) sequences were also published [38]. Based on the previously published results, a combination of several approaches was integrated to sensitively select and determine H5N1 viral protein. Streptavidin-modified paramagnetic particles were mixed with biotinylated selective glycan. Glycan-binding proteins are often expressed by viruses, bacteria, and protozoa on their surfaces to facilitate their attachment to host cells and establish colonization and infection. The first key step in the process of infection, transmission, and virulence of influenza viruses involves HA, a trimeric glycoprotein expressed on the influenza virus membrane [5], which binds to a host cell's surface glycans via a terminal sialic acid (Sia) with α2–3 and α2–6 linkages [39, 40]. A fully automated setup was developed using a pipetting robot as described in Fig. 5. (PCR 96) 10 μL of Dynabeads M-270 Streptavidin were pipetted (Fig. 5A) out of each well of a plate. The plate was then transferred to a magnet plate where the stored solution was extracted from the beads. Beads were washed three times with 100 μL of phosphate buffer (0.3 M; pH 7.4) followed by the addition of 20 μL biotinylated glycan to each well. In the following step, 20 μL of H5N1-Cd-labeled protein was added proceeded by incubation (30 min, 25°C, 400 rpm) and washing with 100 μL of phosphate buffer (0.3 M; pH 7.4) (Fig. 5C). Samples were treated with ultrasound needle (2 min.) (Fig. 5D). The plate was transferred to a magnet, and the product from each well was analyzed using electrochemical analysis. Cadmium was detected by differential pulse voltammetry and H5N1 protein was confirmed present using Brdicka reaction (Fig. 5).

3.5 Optimization of biosensing system parameters

Selected components and their effect were tested to design a biosensor. The influence of varying concentrations of glycan on the amount of isolated H5N1 CdS QDs-viral protein complex was investigated. Changes in cadmium(II) ions peak height showed increasing dependency on the concentration of biotinylated glycan. Thirty-minute treatments with viral protein (5 μg/mL) at 25°C and 400 rpm showed a maximum response with 250 μg/mL of glycan (Fig. 6A). Maximum capacity of particles was not achieved until concentrations reached 1 mg/mL, but this in some biosensing applications is economically disadvantageous. Increasing the surface coverage of coated paramagnetic particles can also be achieved by imposing longer interaction time. Thirty to sixty minutes of incubation treatments (up to 60%), show a dramatic increase in signal as shown in Fig. 6B. The cadmium peaks are shown in Fig. 6B. Treatments lasting 120 min augment the

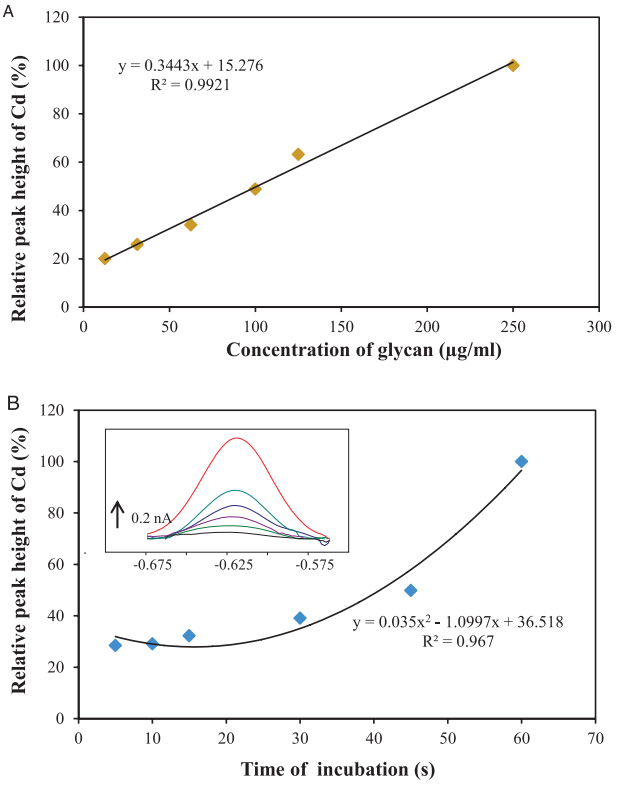

Figure 6. Isolation of complex H5N1-CdS (5 μg/mL) on paramagnetic particles in connection with glycan binding. Influence of (A) glycan concentration and (B) time of interaction on measured cadmium signal; inset: cadmium peaks. For other experimental conditions, see Section 2.

cadmium(II) ion signal by more than 30%. Protein concentrations were also determined using Brdicka reaction. The obtained voltammograms are shown in inset of Fig. 7. Cat2 peak height increased with increasing viral protein concentration (Fig. 7). The greater intercept value of the curve is associated with streptavidin release from paramagnetic particles' surface during ultrasound needle.

3.6 Calibration of the assay

The effects of viral protein concentrations on H5N1 fully automated isolation procedure were monitored. Under optimized conditions (250 μg/mL of glycan, 30-min long interaction, 25°C and 400 rpm), the typical dependence of the cadmium content per mg H5N1 viral protein is shown in Fig. 8. Individual signals of applied varying concentrations (0.625, 1.25, 2.5, 3.75, and 5 μg/mL H5N1-CdS QDs) measured at HMDE (blue rhombus) and GCE (red square) exhibited good linearity, $y = 0.0284x + 0.0054$, with $R^2 = 0.9904$ for HMDE and, $y = 0.024x + 0.0017$, with $R^2 = 0.9923$ for FIA GCE. Detectable amounts of cadmium in the protein were 10 ng per mg, which meant submicrograms quantities of viral protein could be identified.

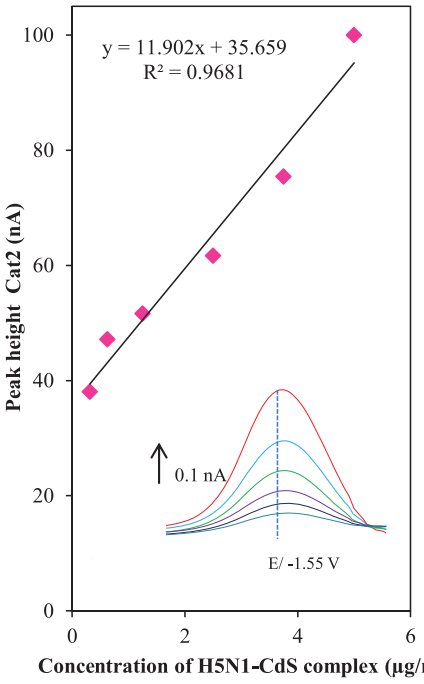

Figure 7. Dependence of Cat2 viral protein H5N1-CdS peak on applied concentration of H5N1 protein; inset: typical voltammograms of Cat2 peal measured at −1.55 V. Volume of measured sample was 3 µL. For other experimental conditions, see Fig. 4.

4 Conclusions

Most cases of human infection due to avian influenza viruses have involved close contact with infected poultry, particularly ill or dying chickens. During the 1997 outbreak in Hong Kong, one case-control study found exposure to live poultry within a week before the onset of illness was associated with human disease, but no significant risk was related to traveling, eating, or preparing poultry products or being exposed to people infected by the H5N1 virus [41]. Effective routine surveillance may be impossible in countries lacking basic public health resources. For a global containment strategy to be successful, low-cost, easy-to-use handheld units that permit decentralized testing are vital. Moreover, a protocol that allows rapid detection of the virus is critical to prevent pandemic spread [42]. A rapid detection method using an automated FIA and particle-based technology in micro-analysis systems may provide laboratories with solutions that enhance laboratory system productivity and test accuracy for the detection of a broad range of disease markers. Techniques using micro- and nanotechnology are used to fabricate lab-on-a-chip devices [43–47]. The paramagnetic particles are modified using biotechnology to make separation and electrochemical detection of viral nucleic acids and proteins easier to measure.

Financial support from NANOSEMED GA AV KAN208130801 and CEITEC CZ.1.05/1.1.00/02.0068 is greatly acknowledged.

The authors have declared no conflict of interest.

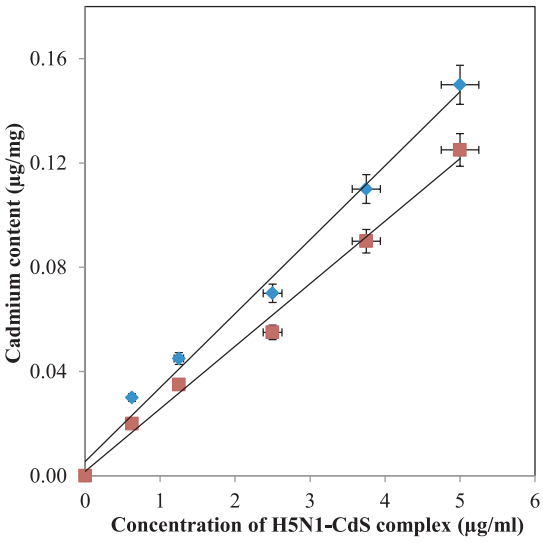

Figure 8. Cadmium content in H5N1-CdS QDs proteins captured on paramagnetic particles determined at (blue rhombus) HMDE and (red square) and FIA-GCE.

5 References

[1] Perdue, M. L., Nguyen, T., *Bull. World Health Organ.* 2012, *90*, 246.

[2] Shindo, N., Briand, S., *Bull. World Health Organ.* 2012, *90*, 247.

[3] Jones, B., *Bull. World Health Organ.* 2012, *90*, 252–253.

[4] WHO, *Bull. WHO* 1980, *58*, 585–591.

[5] Garten, R. J., Davis, C. T., Russell, C. A., Shu, B., Lindstrom, S., Balish, A., Sessions, W. M., Xu, X. Y., Skepner, E., Deyde, V., Okomo-Adhiambo, M., Gubareva, L., Barnes, J., Smith, C. B., Emery, S. L., Hillman, M. J., Rivailler, P., Smagala, J., de Graaf, M., Burke, D. F., Fouchier, R. A. M., Pappas, C., Alpuche-Aranda, C. M., Lopez-Gatell, H., Olivera, H., Lopez, I., Myers, C. A., Faix, D., Blair, P. J., Yu, C., Keene, K. M., Dotson, P. D., Boxrud, D., Sambol, A. R., Abid, S. H., George, K. S., Bannerman, T., Moore, A. L., Stringer, D. J., Blevins, P., Demmler-Harrison, G. J., Ginsberg, M., Kriner, P., Waterman, S., Smole, S., Guevara, H. F., Belongia, E. A., Clark, P. A., Beatrice, S. T., Donis, R., Katz, J., Finelli, L., Bridges, C. B., Shaw, M., Jernigan, D. B., Uyeki, T. M., Smith, D. J., Klimov, A. I., Cox, N. J., *Science* 2009, *325*, 197–201.

[6] Kaleta, E. F., Hergarten, G., Yilmaz, A., *Dtsch. Tierarztl. Wochenschr.* 2005, *112*, 448–456.

[7] Wang, T. T., Parides, M. K., Palese, P., *Science* 2012, *335*, 1463–1463.

[8] Liu, G. D., Wang, J., Wu, H., Lin, Y. Y., Lin, Y. H., *Electroanalysis* 2007, *19*, 777–785.

[9] Dequaire, M., Degrand, C., Limoges, B., *Anal. Chem.* 2000, *72*, 5521–5528.

[10] Gonzalez-Garcia, M. B., Fernandez-Sanchez, C., Costa-Garcia, A., *Biosens. Bioelectron.* 2000, *15*, 315–321.

[11] Wang, J., Xu, D. K., Kawde, A. N., Polsky, R., *Anal. Chem.* 2001, *73*, 5576–5581.

[12] Liu, G. D., Wang, J., Kim, J., Jan, M. R., Collins, G. E., *Anal. Chem.* 2004, *76*, 7126–7130.

[13] Liu, G. D., Lin, Y. H., *Talanta* 2007, *74*, 308–317.

[14] Li, H., Shih, W. Y., Shih, W. H., *Ind. Eng. Chem. Res.* 2007, *46*, 2013–2019.

[15] Long, G. L., Winefordner, J. D., *Anal. Chem.* 1983, *55*, A712–A724.

[16] Chandrasekaran, A., Srinivasan, A., Raman, R., Viswanathan, K., Raguram, S., Tumpey, T. M., Sasisekharan, V., Sasisekharan, R., *Nat. Biotechnol.* 2008, *26*, 107–113.

[17] Stevens, J., Blixt, O., Paulson, J. C., Wilson, I. A., *Nat. Rev. Microbiol.* 2006, *4*, 857–864.

[18] Stevens, J., Corper, A. L., Basler, C. F., Taubenberger, J. K., Palese, P., Wilson, I. A., *Science* 2004, *303*, 1866–1870.

[19] Stevens, J., Blixt, O., Tumpey, T. M., Taubenberger, J. K., Paulson, J. C., Wilson, I. A., *Science* 2006, *312*, 404–410.

[20] Yamada, S., Suzuki, Y., Suzuki, T., Le, M. Q., Nidom, C. A., Sakai-Tagawa, Y., Muramoto, Y., Ito, M., Kiso, M., Horimoto, T., Shinya, K., Sawada, T., Usui, T., Murata, T., Lin, Y. P., Hay, A., Haire, L. F., Stevens, D. J., Russell, R. J., Gamblin, S. J., Skehel, J. J., Kawaoka, Y., *Nature* 2006, *444*, 378–382.

[21] Bewley, C. A., *Nat. Biotechnol.* 2008, *26*, 60–62.

[22] Suenaga, E., Mizuno, H., Penmetcha, K. K. R., *Biosens. Bioelectron.* 2012, *32*, 195–201.

[23] Huska, D., Zitka, O., Krystofova, O., Adam, V., Babula, P., Zehnalek, J., Bartusek, K., Beklova, M., Havel, L., Kizek, R., *Int. J. Electrochem. Sci.* 2010, *5*, 1535–1549.

[24] Kleckerova, A., Sobrova, P., Krystofova, O., Sochor, J., Zitka, O., Babula, P., Adam, V., Docekalova, H., Kizek, R., *Int. J. Electrochem. Sci.* 2011, *6*, 6011–6031.

[25] Krystofova, O., Trnkova, L., Adam, V., Zehnalek, J., Hubalek, J., Babula, P., Kizek, R., *Sensors* 2010, *10*, 5308–5328.

[26] Adam, V., Baloun, J., Fabrik, I., Trnkova, L., Kizek, R., *Sensors* 2008, *8*, 2293–2305.

[27] Petrlova, J., Potesil, D., Mikelova, R., Blastik, O., Adam, V., Trnkova, L., Jelen, F., Prusa, R., Kukacka, J., Kizek, R., *Electrochim. Acta* 2006, *51*, 5112–5119.

[28] Heyrovsky, M., *Electroanalysis* 2000, *12*, 935–939.

[29] Adam, V., Fabrik, I., Eckschlager, T., Stiborova, M., Trnkova, L., Kizek, R., *TRAC-Trends Anal. Chem.* 2010, *29*, 409–418.

[30] Raspor, B., Paic, M., Erk, M., *Talanta* 2001, *55*, 109–115.

[31] Pipper, J., Inoue, M., Ng, L. F. P., Neuzil, P., Zhang, Y., Novak, L., *Nat. Med.* 2007, *13*, 1259–1263.

[32] Chui, L., Drebot, M., Andonov, A., Petrich, A., Glushek, M., Mahony, J., *Diagn. Microbiol. Infect. Dis.* 2005, *53*, 47–55.

[33] Deng, M. J., Long, L., Xiao, X. Z., Wu, Z. X., Zhang, F. J., Zhang, Y. M., Zheng, X. L., Xin, X. Q., Wang, Q., Wu, D. L., *Vet. Immunol. Immunopathol.* 2011, *141*, 183–189.

[34] Mizutani, H., Suzuki, M., Fujiwara, K., Shibata, S., Arishima, K., Hoshino, M., Ushijima, H., Honma, H., Kitamura, T., *Microbiol. Immunol.* 1991, *35*, 717–727.

[35] Bonnafous, P., Perrault, M., Le Bihan, O., Bartosch, B., Lavillette, D., Penin, F., Lambert, O., Pecheur, E. I., *J. Gen. Virol.* 2010, *91*, 1919–1930.

[36] Lien, K. Y., Hung, L. Y., Huang, T. B., Tsai, Y. C., Lei, H. Y., Lee, G. B., *Biosens. Bioelectron.* 2011, *26*, 3900–3907.

[37] Chou, T. C., Hsu, W., Wang, C. H., Chen, Y. J., Fang, J. M., *J. Nanobiotechnol.* 2011, *9*, 52.

[38] Lim, S. H., Bestvater, F., Buchy, P., Mardy, S., Yu, A. D. C., *Sensors* 2009, *9*, 5590–5599.

[39] Skehel, J. J., Wiley, D. C., *Annu. Rev. Biochem.* 2000, *69*, 531–569.

[40] Russell, R. J., Kerry, P. S., Stevens, D. J., Steinhauer, D. A., Martin, S. R., Gamblin, S. J., Skehel, J. J., *Proc. Natl. Acad. Sci. USA* 2008, *105*, 17736–17741.

[41] Hayden, F., Croisier, A., *J. Infect. Dis.* 2005, *192*, 1311–1314.

[42] Adam, V., Huska, D., Hubalek, J., Kizek, R., *Microfluid. Nanofluid.* 2010, *8*, 329–339.

[43] Manz, A., Graber, N., Widmer, H. M., *Sens. Actuator B-Chem.* 1990, *1*, 244–248.

[44] Janasek, D., Franzke, J., Manz, A., *Nature* 2006, *442*, 374–380.

[45] Kizek, R., Masarik, M., Kramer, K. J., Potesil, D., Bailey, M., Howard, J. A., Klejdus, B., Mikelova, R., Adam, V., Trnkova, L., Jelen, F., *Anal. Bioanal. Chem.* 2005, *381*, 1167–1178.

[46] Masarik, M., Kizek, R., Kramer, K. J., Billova, S., Brazdova, M., Vacek, J., Bailey, M., Jelen, F., Howard, J. A., *Anal. Chem.* 2003, *75*, 2663–2669.

[47] Hubalek, J., Adam, V., Kizek, R., in: Conley, E. C., Dini, P., Doarn, C., Holopainen, A. (Eds.), *International Conference on eHealth, Telemedicine, and Social Medicine, eTELEMED*, Institute of Electrical and Electronics Engineers (IEEE), Cancun, Mexico 2009, pp. 108–112, Article 4782641.

